

# Dynamic Bayesian Network Modeling of Hippocampal Subfields Connectivity with 7T fMRI: A Case Study

Fernando P. Santos<sup>1</sup>, Stephen F. Smagula<sup>2</sup>, Helmet Karim<sup>3</sup>, Tales S. Santini<sup>3</sup>, Howard J. Aizenstein<sup>2</sup>, Tamer S. Ibrahim<sup>3,4</sup> and Carlos D. Maciel<sup>1</sup>

<sup>1</sup>*Department of Electrical Engineering, São Carlos School of Engineering, University of São Paulo, Av. Trabalhador Saocarlense, 400, 13561010, São Carlos, São Paulo, Brazil*

<sup>2</sup>*Department of Psychiatry, Western Psychiatric Institute and Clinic, University of Pittsburgh School of Medicine, 3811 O'Hara Street, 15213, Pittsburgh, Pennsylvania, U.S.A.*

<sup>3</sup>*Department of Bioengineering, University of Pittsburgh, 3700 O'Hara Street, 15213, Pittsburgh, Pennsylvania, U.S.A.*

<sup>4</sup>*Department of Radiology, University of Pittsburgh, 200 Lothrop Street, 15213, Pittsburgh, Pennsylvania, U.S.A*

**Keywords:** Dynamic Bayesian Networks, fMRI, Network Modelling, Hippocampus.

**Abstract:** The development of high resolution structural and functional magnetic resonance imaging, along with the new automatic segmentation procedures for identifying brain regions with high precision and level of detail, has made possible new studies on functional connectivity in the medial temporal lobe and hippocampal subfields, with important applications in the understanding of human memory and psychiatric disorders. Many previous analyses using high resolution data have focused on undirected measures between these subfields. Our work expands this by presenting Dynamic Bayesian Network (DBN) models as an useful tool for mapping directed functional connectivity in the hippocampal subfields. Besides revealing directional connections, DBNs use a model-free approach which also exclude indirect connections between nodes of a graph by means of conditional probability distribution. They also relax the constraint of acyclicity imposed by traditional Bayesian networks (BNs) by considering nodes at different time points through a Markovianity assumption. We apply the GlobalMIT DBN learning algorithm to one subject with fMRI time-series obtained from three regions: the cornu ammonis (CA), dentate gyrus (DG) and entorhinal cortex (ERC), and find an initial network structure, which can be further expanded with the inclusion of new regions and analyzed with a group analysis method.

## 1 INTRODUCTION

Establishing functional connectivity networks in the brain has become a major focus with the advance of neuroimaging techniques such as electroencephalography (EEG), magnetoencephalography (MEG), and functional magnetic resonance imaging (fMRI) (Wang et al., 2015; Smith et al., 2011). Specifically, fMRI presents advantages as it has high spatial resolution, allowing connectivity studies to focus on very specific parts of the brain including deeper brain structures not accessible by MEG or EEG. Therefore, one of the areas receiving attention in recent years is the hippocampal sub-fields and more specifically their connectivity. The hippocampus is a structure located in the medial temporal lobe (MTL) and has been associated with learning and memory (Jeneson and Squire, 2012). Alterations in its structure and connectivity are shown to be associated with

several neurological and psychiatric disorders such as Alzheimer's disease, epilepsy, schizophrenia, and others (Bartsch, 2012). Studies have been stressing the importance of considering the hippocampal sub-structures for a better understanding of its function and pathologies, instead of considering it as a whole (Maruszak and Thuret, 2015). However due to the low resolution of the fMRI data, this type of analysis was not possible on the hippocampus sub-fields, and only recently, with the newest advances on ultra-high field MRI with 7T scanners, higher-resolution images are being obtained and analyzed (Duyn, 2012). Moreover, advances in automatic segmentation procedures also facilitate the extraction of regions of interest (ROIs) and the usage of more data, since manual segmentation may be very time consuming and prone to errors (Wisse et al., 2016; Yushkevich et al., 2015). Recently, studies have demonstrated functional subdivisions of the medial temporal lobe along the longitu-

dinal axis of the hippocampus (Libby et al., 2012), between hippocampal and para-hippocampal structures (Libby et al., 2012; Das et al., 2013), and across sub-fields (Lacy and Stark, 2012; de Flores et al., 2015).

Among the methods for brain connectivity, (Friston, 2011) has divided types of connectivity into functional and effective connectivity, with the first describing "statistical dependencies among remote neurophysiological events", while the second describes "the influence that one neural system exerts over another, either at a synaptic or population level". A spectrum of methods exist that fall between these two approaches, with effective connectivity having more complex and biologically informed models, used for a confirmatory approach, while functional connectivity presents simpler and more generic methods, used for an exploratory approach (i.e., network discovery) (Valdes-Sosa et al., 2011). The direction of the connections between nodes is also an important factor — and in fact, recent work by (Li et al., 2013) reveals alterations of directional connectivity in patients with Alzheimer disease, pointing to the importance of this kind of knowledge in clinical analysis. (Smith et al., 2011) also notes this, and separates methods capable of describing directional connectivity in three categories: *lag-based* methods (Rodrigues and Andrade, 2014, See review in), such as Granger causality (Granger, 1969); *conditional independence* methods, such as Bayesian networks (BN) (Mumford and Ramsey, 2014) and Dynamic Causal Modeling (DCM) (Friston et al., 2003), and *higher-order statistics*, such as Patel's pairwise conditional probability approach (Patel et al., 2006).

Dynamic Bayesian Networks (DBNs) can be regarded as a directed functional connectivity approach (and thus, are used for exploratory analyses, instead of confirmatory, such as DCM) that overcomes the limitations of acyclicity imposed by the traditional Bayesian network framework. They are Bayesian networks with nodes representing the processes at different time points, given a Markovianity assumption; thus, cycles may be present as a result of temporal dynamics. Besides, the Bayesian network framework is able to differentiate direct from indirect connections (or, marginal dependences) between nodes by means of conditional probabilities (Valdes-Sosa et al., 2011). DBNs were applied to fMRI data in many studies (Ide et al., 2014; Bielza and Larrañaga, 2014) and were modeled either with discrete data (with the conditional probability distributions (CPD) are represented by a probability table) (Rajapakse and Zhou, 2007; Burge et al., 2009) or with continuous data through a gaussianity assumption (Zhang et al., 2005; Chen et al., 2012; Wu et al., 2014). The advantage of the

first case is that nonlinear processes are better modeled, at the cost of reducing the original signal to discrete values and requiring more samples, while in the second case, processes are considered linear, but don't have to be discretized.

From the fact that the current state of knowledge in hippocampal sub-fields connectivity and availability of data demands an exploratory approach, this study used DBNs as a tool for finding directed functional connectivity between the hippocampal sub-fields of the a resting state brain. This helps advance current knowledge on the function of the medial temporal lobe by introducing information on the direction of the connections, instead of only undirected and pairwise correlations between regions. The model is learned by an algorithm based on the search and score paradigm, and uses the mutual information criterion (MIT) (de Campos, 2006; Vinh et al., 2011a) to evaluate the goodness-of-fit of a DBN structure to the data employed. Time-series data is obtained by extracting average ROI time-series from the BOLD fMRI data with coregistered hippocampal sub-field labels obtained through an automatic segmentation algorithm applied to structural T1 and T2-weighted structural images. The highest scoring DBN structure found for one subject shows the use of DBNs as a promising way to map the directed functional connectivity of medial temporal lobe sub-structures using ultra-high resolution neuroimaging.

## 2 METHODS

### 2.1 MRI Data

Images were collected from older adults diagnosed with late-life depression, at the Department of Radiology of University of Pittsburgh (NIH Project number 1R01MH11265-01). Scanning was done on a 7T human MRI system (Magnetom, Siemens Medical Systems, Erlangen, Germany) with a 20-to-8-channel transmit and 32-channel adjustable receive coil (Ibrahim et al., 2013).

Structural T1 and T2-weighted images were used for identifying the subregions with the automatic segmentation. An axial, whole-brain T1 was obtained with a Magnetization Prepared Rapid Gradient Echo (MPRAGE) sequence with 3D orientation, isotropic resolution 0.7mm<sup>3</sup> and parameters TR/TI/TE=3000/1200/2.47 ms, 6 flip angle, FoV=192 × 220, 280 × 320 acquisition matrix and an acquisition time 10 min and 31 s. Axial, whole-brain T2-weighted images used a 3D Turbo Spin Echo (TSE) sequence with 0.37 × 0.37mm in plane reso-

lution and 1.5mm slice thickness; parameters were TR/TE=7900/56 ms, 130 flip angle, FoV=165 × 189, 32 interleaved slices and acquisition time 5 min and 25 s. Finally, 4D axial, whole-brain (excluding the cerebellum) BOLD fMRI data were acquired with a gradient echo planar (EPI) sequence with 155 time points and 2.3mm isotropic voxel size, 46 interleaved slices, TR/TE=2500/20 ms, 70 flip angle, FoV=1546 × 1546, 96 × 96 acquisition matrix and acquisition time 6 min and 27 s. Patients rested with eyes open and lights off.

## 2.2 Segmentation and Preprocessing

Three ROIs are considered in the model: the dentate gyrus (DG), the four fields of the cornu ammonis (CA14) (considered as one) and the entorhinal cortex (ERC) from only one hemisphere of a subject (Bartsch, 2012, See). The reason for choosing only these is that as the number of nodes included in a DBN model grows, the number of time points needed for learning need to grow as well (Koller and Friedman, 2009) — and, with one subject, only 155 time points are available. The ROIs are identified in the T2-weighted images using an automatic segmentation procedure applied to the images using the ASHS software developed by (Yushkevich et al., 2015). ASHS uses a multi-atlas label fusion approach for obtaining the hippocampal subfields with T1 and T2-weighted images (For a review of methods, see Dill et al., 2015). A 7T atlas, based on images obtained in the PREDICT-MR study (Wisse et al., 2014), tested with ASHS in (Wisse et al., 2016) and made available publicly, was used.

Preprocessing and image registering was done with the statistical parametric mapping software (SPM12) (Penny et al., 2011). Functional images were slice-time corrected (reference slice was the temporally middle slice with sinc interpolation), motion corrected (mean scan was used as reference with mutual information as the similarity metric and 4th degree B-spline interpolation), and smoothed with a Gaussian smoothing kernel (FWHM of 8mm). The T2-weighted images and segmentation labels are registered and resliced to match the functional image. Time-series from the voxels of the ROIs are extracted from the functional image according the aligned segmentation labels. A mean intensity normalization is applied: the average value of the ROI in each time point is subtracted from each time-series, and normalization is applied, with values ranging from -1 to 1. Time-series of each ROIs are then averaged, yielding one time-series for each ROI (Ide et al., 2014).

Time-series extracted from the ROIs are usually

non-stationary and present DC level trends that hinder the ability to use sequential time points for training a DBN (i.e., the supposition of ergodicity). These trends are usually considered irrelevant to the model and thus are removed by linear detrending methods (Ide et al., 2014) and normalization. However, one must consider the possibility that these trends can be non-linear and present discontinuities, so that traditional detrending methods may not achieve stationary time-series. Therefore, the Singular Spectrum Analysis (SSA) technique is an interesting option due to its model-free characteristic and ability to remove complex trends (i.e., not just linear or quadratic) and discontinuities with very few specification parameters (Golyandina and Zhigljavsky, 2013). We employ this technique in the present work, by applying to each time-series obtained from the ROIs. SSA's main idea is to "decompose the original series into the sum of a small number of independent and interpretable components such as a slowly varying trend, oscillatory components and structure-less noise" (Hassani, 2007) and reconstruct it according to the components desired — in case, the lowest oscillatory components (which can be regarded as containing the direct current (DC) level), represented by the largest eigenvalues obtained in the Singular Value Decomposition (SVD) of the time-series' embedding matrix (Golyandina and Zhigljavsky, 2013).

## 2.3 Learning Discrete Dynamic Bayesian Networks

We start by defining a Dynamic Bayesian Network (DBN). Let  $\mathbf{X}^{(t)} = \{X_1^{(t)}, X_2^{(t)}, \dots, X_N^{(t)}\}$  be a set of  $N$  time-series of length  $T$ , where  $X_i^{(t)}$  is a random variable representing the process  $X_i$  at time slice  $t$ . A DBN models the joint probability distribution  $\mathbf{X}^{(1)} \cup \mathbf{X}^{(2)} \dots \cup \mathbf{X}^{(T)}$  by means of a directed acyclic graph (DAG)  $G$  encoding the conditional independences between the random variables of the system (Friedman et al., 1998). Three assumptions are made: (1) first order Markovianity, i.e.,  $\forall t, (\mathbf{X}^{(t+1)} \perp \mathbf{X}^{(0:t-1)} | \mathbf{X}^{(t)})$ , (2) stationarity, i.e.,  $P(\mathbf{X}^{(t)} | \mathbf{X}^{(t-1)})$  is independent of  $t$ , and (3) Markov causal condition, i.e.,  $(X_i^{(t)} \perp \mathbf{Nd}(X_i^{(t)}) | \mathbf{Pa}(X_i^{(t)}))$ , where  $\mathbf{Nd}(X_i^{(t)})$  are the non-descendant nodes of  $X_i^{(t)}$ , and  $\mathbf{Pa}(X_i^{(t)})$  are the parent nodes of  $X_i^{(t)}$  in the DAG  $G$  (Neapolitan et al., 2004). Thus, this permits the decomposition of the joint probability distribution of all the processes of the system as:

$$P(\mathbf{X}^{(0:t)}) = P(\mathbf{X}^{(0)}) \prod_{t=1}^T P(\mathbf{X}^{(t)} | \mathbf{X}^{(t-1)}) \quad (1)$$

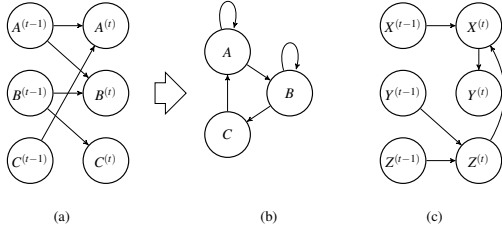


Figure 1: Examples of DBNs. (a) presents a DBN with only inter time-slice edges, which can be represented as a cyclic graph as shown in (b) (used in the present study). (c) presents a DBN with both intra and inter time-slice edges.

and the further decomposition of the joint transition probability  $P(\mathbf{X}^{(t)}|\mathbf{X}^{(t-1)})$  as:

$$P(\mathbf{X}^{(t)}|\mathbf{X}^{(t-1)}) = \prod_{i=1}^N P(X_i^{(t)}|\mathbf{Pa}(X_i^{(t)})) \quad (2)$$

These decompositions thus permit both network inference algorithms for unknown variables and the formulation of scoring metrics and other structure learning procedures from data (such as the one used and presented further) (Neapolitan et al., 2004).

DBNs can include edges between nodes in a same time slice  $t$  (intra time slice) and between time slices  $t-1$  and  $t$  (inter time slice) (time slices  $t-2$  and on can be included by relaxing the Markovianity assumption to permit higher orders, such as in (Xuan et al., 2012) and (Santos and Maciel, 2014)). Figure 1 (c) illustrates this type of network. However, for simplicity, many authors consider DBNs including only inter time slice edges (Xuan et al., 2012; Smith et al., 2006). This last case permits an equivalent graph representation without specifying time-series at different time points and thus without the acyclicity restriction, such as shown in Figure 1(a,b).

DBN graphs can be learned from data through many approaches, among which are conditional independence tests, score metrics, and model averaging (such as Markov Chain Monte Carlo) (Koller and Friedman, 2009). In this paper we employ the score metrics approach for discrete models (dDBNs), in which, after searching through a space of possible graph structures, a scoring function determines how good this structure is given the data. Particularly, we employ the GlobalMIT method, implemented in a Matlab/C++ toolkit (Vinh et al., 2011a). GlobalMIT adapts the MIT scoring metric proposed by (de Campos, 2006), devised initially for static Bayesian networks, to DBNs and uses an optimized search algorithm operating under polynomial time (Vinh et al., 2011b). The MIT scoring metric evaluates the goodness-of-fit of a network "as the total mutual information shared between each node and its

parents, penalized by a term which quantifies the degree of statistical significance of this shared information" (Xuan et al., 2012), and was shown to compete favorably with other scoring metrics such as Bayesian Dirichlet equivalence (BDe) and Bayesian Information Criterion (BIC) (de Campos, 2006). For a candidate graph  $G$  with  $N$  nodes and their corresponding  $\{r_1, \dots, r_n\}$  discrete states, and a dataset  $D$  with  $N_D$  observations, the MIT score is defined as (de Campos, 2006):

$$S_{MIT}(G : D) = \sum_{\substack{i=1 \\ \mathbf{Pa}(X_i) \neq \emptyset}}^N \{2N_D \cdot I(X_i, \mathbf{Pa}(X_i)) - \sum_{j=1}^{s_i} \chi_{\alpha, l_{i\sigma_i(j)}}\} \quad (3)$$

where  $I(X_i, \mathbf{Pa}(X_i))$  is the mutual information between  $X_i$  and its parents, and  $\chi_{\alpha, l_{i\sigma_i(j)}}$  is the value such that  $p(\chi^2(l_{i,j}) \leq \chi_{\alpha, l_{i,j}}) = \alpha$  (the chi-square distribution at significance level  $1 - \alpha$ , with the term  $l_{i\sigma_i(j)}$  defined as:

$$l_{i\sigma_i(j)} = \begin{cases} (r_i - 1)(r_{i\sigma_i(j)} - 1) \prod_{k=1}^{j-1} r_{i\sigma_i(k)}, & j = 2, \dots, s_i \\ (r_i - 1)(r_{i\sigma_i(j)} - 1), & j = 1 \end{cases} \quad (4)$$

where  $\sigma_i = \{\sigma_i(1), \dots, \sigma_i(s_i)\}$  is any permutation of the index set  $\{1, \dots, s_i\}$  of  $\mathbf{Pa}(X_i)$ , with the first variable having the greatest number of states, the second having the second, and so on.

The GlobalMIT algorithm then investigates, for each node, every potential parent set of increasing cardinality until the globally optimal solution is found. This guarantees a polynomial worst-case time complexity, given the assumptions that the DBN includes only inter time slices (thus eliminating the necessity of checking acyclicity of candidate graphs) and variables have the same number of discrete states (considering also the MIT scoring criterion is used in the algorithm) (Vinh et al., 2011a). GlobalMIT is also deterministic, and thus have advantage over stochastic global optimization methods, since it does not get stuck in local minima (Vinh et al., 2011b). The algorithm also uses the following decomposition property of mutual information:

$$I(X_i, \mathbf{Pa}(X_i) \cup X_j) = I(X_i, \mathbf{Pa}(X_i)) + I(X_i, X_j | \mathbf{Pa}(X_i)) \quad (5)$$

which permits an incremental calculation of mutual information, with cached intermediary values to prevent redundant computation, and thus a better efficiency.

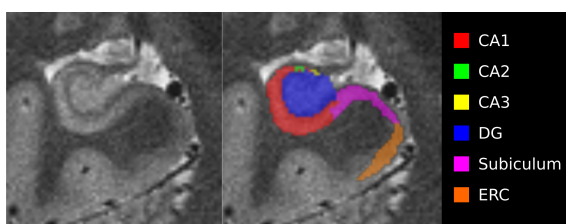


Figure 2: Resulting labels from the automatic segmentation procedure implemented in ASHS (Yushkevich et al., 2015). Labels are shown at the T2-weighted structural image with 0.x0.x0. mm, but are afterwards registered to the functional images for the ROI time-series extraction procedure and network learning.



Figure 3: Highest scoring DBN structure with the GlobalMIT score applied to the hippocampal subfields nodes. CA stands for cornu ammonis; DG, dentate gyrus and ERC, entorhinal cortex.

### 3 RESULTS AND DISCUSSION

Automatic segmentation of hippocampal sub-fields was applied to T1 and T2-weighted images of one subject, as shown in Figure 2. After the registrations and preprocessing, three ROI time-series were extracted and from the fMRI image: CA, DG and ERC. Then, SSA technique was applied to remove complex trends in the signals - time-series were decomposed into 50 components, and 2 of the lowest oscillatory components (related to the largest eigenvalues of the SVD decomposition) were removed. Finally, data were discretized to 5 bins ( $d = 5$ ) and the GlobalMIT algorithm was applied for obtaining the discrete DBN structure. After structure search, the high scoring graph was the one presented in Figure 3, with significance level of  $\alpha = 0.95$ .

The network structure found reveals a mutual connection between CA and DG fields and a directed connection from DG to ERC. This indicates that the connection between CA and ERC is mediated by the DG, and this finding may explain why the DG is more functionally connected to the parahippocampal and cingulate cortices than the CA (de Flores et al., 2015) ((Libby et al., 2012) shows that connections between the hippocampal subfields and the parahippocampal cortex are mediated by the ERC). A fuller understanding of these connections, however, would require an analysis at group level, since this reflects results found for one subject.

### 4 CONCLUSION & FUTURE WORK

Advances with ultra-field MRI, yielding high-resolution fMRI data, and automatic segmentation procedures for sub-field identification are opening the way for studies on sub-field level connectivity analyses in the brain. In this study, we demonstrated the feasibility of a directed functional connectivity analysis of hippocampal sub-fields data obtained with ultra-high resolution neuroimaging, automatic segmentation and DBN models. The resulting DBN models are able to identify direction of connections and differentiate direct from indirect connections between ROIs, which may better explain the function of each hippocampal sub-field. Also, in the preprocessing steps, we included a novel application of the SSA technique for removing complex trends and discontinuities from time-series in a flexible, model-free way and with very few specification parameters.

Results, however, were obtained for only one subject, and thus the next step of work will be a group level analysis, including data from multiple subjects, for a more complete interpretation of results. DBN group analysis techniques are described in (Li et al., 2007) and (Li et al., 2008), in which three main groups are distinguished: "the virtual-typical-subject (VTS) approach which pools or averages group data as if they are sampled from a single, hypothetical virtual typical subject; the individual-structure (IS) approach that learns a separate BN for each subject, and then finds commonality across the individual structures, and the common-structure (CS) approach that imposes the same network structure on the BN of every subject, but allows the parameters to differ across subjects" (Li et al., 2008). An investigation of inter-subject conformities and variations can yield important results for functional and clinical studies (Bielza and Larrañaga, 2014) on the hippocampus and medial temporal lobe, such as identification of early stages of progression of Alzheimer's disease (Das et al., 2013).

Another future step consists in including more ROIs, for a more complete network model — until now, usage of data of only one subject (thus, with only 155 time points) limits the number of nodes to be included in the network. Important regions to be added are the remaining parts of the medial temporal lobes — the subiculum (part of the hippocampus), the perirhinal cortex (PRC) and the parahippocampal cortex (PHC)— and also the anterior and posterior cingulate cortices; all of these from both the right and left hemispheres, as investigated in previous work such as (Lacy and Stark, 2012) and (de Flores et al., 2015). A study with a seed-to-voxel correlation analysis will

be also conducted for identifying relevant activation areas to be included (such as described in (Ide et al., 2014)).

Requirements of data for learning DBNs can be naturally overcome with some types of analysis at group level — (Burge et al., 2009), for example, employs a cross-validation procedure, including data from multiple subjects. The requirements can also be overcome by means of multi-modal learning techniques, which use data from multiple types of images to reduce the search space of networks or models. (Schulz et al., 2004), for example, performs an integrated MEG and fMRI for connectivity analysis, (Rykhlevskaia et al., 2008) performs a survey of methods integrating structural and functional images for connectivity analysis, and (Zhu et al., 2014) surveys of methods integrating diffusion tensor imaging (DTI) with functional images. (Iyer et al., 2013), for example, uses DTI data as a baseline matrix for an Bayesian network structure learning procedure — an important insight that may be further incorporated.

## ACKNOWLEDGEMENTS

This work was supported by grants T32 MH019986 and P30 MH090333 from the National Institutes of Health (USA), grant 2016/02621-0 from So Paulo Research Foundation (FAPESP/Brazil), grant 475064/2013-5 from National Council of Technological and Scientific Development (CNPq/Brazil), and grant BEX 13385/13-5 from Capes Foundation (Brazil).

## REFERENCES

- Bartsch, T. (2012). *The clinical neurobiology of the hippocampus: An integrative view*, volume 151. Oxford University Press.
- Bielza, C. and Larrañaga, P. (2014). Bayesian networks in neuroscience: a survey. *Frontiers in computational neuroscience*, 8:131.
- Burge, J., Lane, T., Link, H., Qiu, S., and Clark, V. P. (2009). Discrete dynamic bayesian network analysis of fmri data. *Human brain mapping*, 30(1):122–137.
- Chen, R., Resnick, S. M., Davatzikos, C., and Herskovits, E. H. (2012). Dynamic bayesian network modeling for longitudinal brain morphometry. *NeuroImage*, 59(3):2330 – 2338.
- Das, S. R., Pluta, J., Mancuso, L., Kliot, D., Orozco, S., Dickerson, B. C., Yushkevich, P. A., and Wolk, D. A. (2013). Increased functional connectivity within medial temporal lobe in mild cognitive impairment. *Hippocampus*, 23(1):1–6.
- de Campos, L. M. (2006). A scoring function for learning bayesian networks based on mutual information and conditional independence tests. *J. Mach. Learn. Res.*, 7:2149–2187.
- de Flores, R., Mutlu, J., Bejanin, A., Tomadesso, C., Landeau, B., Mézence, F., de La Sayette, V., Eustache, F., and Chételat, G. (2015). Intrinsic connectivity of hippocampal subfields in normal elderly and its disturbance in mci patients. *Alzheimer's & Dementia: The Journal of the Alzheimer's Association*, 11(7):P61.
- Duyn, J. H. (2012). The future of ultra-high field {MRI} and fmri for study of the human brain. *NeuroImage*, 62(2):1241 – 1248. 20 {YEARS} {OF} fMRI20 {YEARS} {OF} fMRI.
- Friedman, N., Murphy, K., and Russell, S. (1998). Learning the structure of dynamic probabilistic networks. In *Proceedings of the Fourteenth conference on Uncertainty in artificial intelligence*, pages 139–147. Morgan Kaufmann Publishers Inc.
- Friston, K. J. (2011). Functional and effective connectivity: a review. *Brain connectivity*, 1(1):13–36.
- Friston, K. J., Harrison, L., and Penny, W. (2003). Dynamic causal modelling. *Neuroimage*, 19(4):1273–1302.
- Golyandina, N. and Zhigljavsky, A. (2013). *Singular Spectrum Analysis for Time Series*. SpringerBriefs in Statistics. Springer.
- Granger, C. W. (1969). Investigating causal relations by econometric models and cross-spectral methods. *Econometrica: Journal of the Econometric Society*, pages 424–438.
- Hassani, H. (2007). Singular spectrum analysis: methodology and comparison. *Journal of Data Science*, 5(2):239–257.
- Ibrahim, T. S., Zhao, Y., Krishnamurthy, N., Raval, S. B., Zhao, T., Wood, S., and Kim, J. (2013). 20-to-8 channel tx array with 32-channel adjustable receive-only insert for 7t head imaging. In *The 21th ISMRM Annual Meeting*, page 4408.
- Ide, J. S., Zhang, S., and Chiang-shan, R. L. (2014). Bayesian network models in brain functional connectivity analysis. *International Journal of Approximate Reasoning*, 55(1):23–35.
- Iyer, S. P., Shafran, I., Grayson, D., Gates, K., Nigg, J. T., and Fair, D. A. (2013). Inferring functional connectivity in mri using bayesian network structure learning with a modified pc algorithm. *Neuroimage*, 75:165–175.
- Jenison, A. and Squire, L. R. (2012). Working memory, long-term memory, and medial temporal lobe function. *Learning & Memory*, 19(1):15–25.
- Koller, D. and Friedman, N. (2009). *Probabilistic graphical models: principles and techniques*. MIT press.
- Lacy, J. W. and Stark, C. E. (2012). Intrinsic functional connectivity of the human medial temporal lobe suggests a distinction between adjacent mtl cortices and hippocampus. *Hippocampus*, 22(12):2290–2302.
- Li, J., Wang, Z. J., and McKeown, M. J. (2007). A framework for group analysis of fmri data using dynamic bayesian networks. In *2007 29th Annual International Conference of the IEEE Engineering in Medicine and Biology Society*, pages 5991–5994. IEEE.

- Li, J., Wang, Z. J., Palmer, S. J., and McKeown, M. J. (2008). Dynamic bayesian network modeling of fmri: a comparison of group-analysis methods. *Neuroimage*, 41(2):398–407.
- Li, R., Wu, X., Chen, K., Fleisher, A., Reiman, E., and Yao, L. (2013). Alterations of directional connectivity among resting-state networks in alzheimer disease. *American Journal of Neuroradiology*, 34(2):340–345.
- Libby, L. A., Ekstrom, A. D., Ragland, J. D., and Ranganath, C. (2012). Differential connectivity of perirhinal and parahippocampal cortices within human hippocampal subregions revealed by high-resolution functional imaging. *The Journal of Neuroscience*, 32(19):6550–6560.
- Maruszak, A. and Thuret, S. (2015). Why looking at the whole hippocampus is not enough: a critical role for anteroposterior axis, subfield and activation analyses to enhance predictive value of hippocampal changes for alzheimers disease diagnosis. *2015: Which new directions for Alzheimer's disease?*, page 6.
- Mumford, J. A. and Ramsey, J. D. (2014). Bayesian networks for fmri: a primer. *Neuroimage*, 86:573–582.
- Neapolitan, R. E. et al. (2004). Learning bayesian networks.
- Patel, R. S., Bowman, F. D., and Rilling, J. K. (2006). A bayesian approach to determining connectivity of the human brain. *Human brain mapping*, 27(3):267–276.
- Penny, W. D., Friston, K. J., Ashburner, J. T., Kiebel, S. J., and Nichols, T. E. (2011). *Statistical parametric mapping: the analysis of functional brain images*. Academic press.
- Rajapakse, J. C. and Zhou, J. (2007). Learning effective brain connectivity with dynamic bayesian networks. *Neuroimage*, 37(3):749–760.
- Rykhlevskaia, E., Gratton, G., and Fabiani, M. (2008). Combining structural and functional neuroimaging data for studying brain connectivity: a review. *Psychophysiology*, 45(2):173–187.
- Santos, F. P. and Maciel, C. D. (2014). A pso approach for learning transition structures of higher-order dynamic bayesian networks. In *Biosignals and Biorobotics Conference (2014): Biosignals and Robotics for Better and Safer Living (BRC), 5th ISSNIP-IEEE*, pages 1–6.
- Schulz, M., Chau, W., Graham, S. J., McIntosh, A. R., Ross, B., Ishii, R., and Pantev, C. (2004). An integrative meg-fmri study of the primary somatosensory cortex using cross-modal correspondence analysis. *NeuroImage*, 22(1):120–133.
- Smith, S. M., Miller, K. L., Salimi-Khorshidi, G., Webster, M., Beckmann, C. F., Nichols, T. E., Ramsey, J. D., and Woolrich, M. W. (2011). Network modelling methods for fmri. *Neuroimage*, 54(2):875–891.
- Smith, V. A., Yu, J., Smulders, T. V., Hartemink, A. J., and Jarvis, E. D. (2006). Computational inference of neural information flow networks. *PLoS computational biology*, 2(11):e161.
- Valdes-Sosa, P. A., Roebroek, A., Daunizeau, J., and Friston, K. (2011). Effective connectivity: influence, causality and biophysical modeling. *Neuroimage*, 58(2):339–361.
- Vinh, N. X., Chetty, M., Coppel, R., and Wangikar, P. P. (2011a). Globalmit: learning globally optimal dynamic bayesian network with the mutual information test criterion. *Bioinformatics*, 27(19):2765–2766.
- Vinh, N. X., Chetty, M., Coppel, R., and Wangikar, P. P. (2011b). Polynomial time algorithm for learning globally optimal dynamic bayesian network. In *International Conference on Neural Information Processing*, pages 719–729. Springer.
- Wang, C., Xu, J., Zhao, S., and Lou, W. (2015). Graph theoretical analysis of eeg effective connectivity in vascular dementia patients during a visual oddball task. *Clinical Neurophysiology*.
- Wisse, L., Kuijf, H., Honingh, A., Wang, H., Pluta, J., Das, S., Wolk, D., Zwanenburg, J., Yushkevich, P., and Geerlings, M. (2016). Automated hippocampal subfield segmentation at 7t mri. *American Journal of Neuroradiology*.
- Wisse, L. E., Biessels, G. J., Heringa, S. M., Kuijf, H. J., Luijten, P. R., Geerlings, M. I., Group, U. V. C. I. V. S., et al. (2014). Hippocampal subfield volumes at 7t in early alzheimer's disease and normal aging. *Neurobiology of aging*, 35(9):2039–2045.
- Wu, X., Wen, X., Li, J., and Yao, L. (2014). A new dynamic bayesian network approach for determining effective connectivity from fmri data. *Neural Computing and Applications*, 24(1):91–97.
- Xuan, N., Chetty, M., Coppel, R., and Wangikar, P. P. (2012). Gene regulatory network modeling via global optimization of high-order dynamic bayesian network. *BMC bioinformatics*, 13(1):131.
- Yushkevich, P. A., Pluta, J. B., Wang, H., Xie, L., Ding, S.-L., Gertje, E. C., Mancuso, L., Kliot, D., Das, S. R., and Wolk, D. A. (2015). Automated volumetry and regional thickness analysis of hippocampal subfields and medial temporal cortical structures in mild cognitive impairment. *Human brain mapping*, 36(1):258–287.
- Zhang, L., Samaras, D., Alia-Klein, N., Volkow, N., and Goldstein, R. (2005). Modeling neuronal interactivity using dynamic bayesian networks. In *Advances in neural information processing systems*, pages 1593–1600.
- Zhu, D., Zhang, T., Jiang, X., Hu, X., Chen, H., Yang, N., Lv, J., Han, J., Guo, L., and Liu, T. (2014). Fusing dti and fmri data: a survey of methods and applications. *Neuroimage*, 102:184–191.